

Cardiac imaging in RASopathies/mitogen activated protein kinase syndromes

Rita Gravino, Giuseppe Pacileo

UOSD Cardiologia Riabilitativa Intensiva e Scompenso, Seconda Università di Napoli, Ospedale Monaldi, Napoli, Italy

Abstract

RASopathies include a spectrum of disorders due to dysregulation of RAS/mitogen activated protein kinase pathway that plays an essential role in the control of the cell cycle and differentiation. As a consequence, its dysregulation has profound developmental consequences, in particular cardiac malformations. *RASopathies* with cardiac features are: Noonan syndrome, multiple lentiginos syndrome, cardio-facio-cutaneous syndrome, Costello syndrome, neurofibromatosis-1, Legius syndrome, neurofibromatosis-Noonan syndrome. The former syndromes are associated with a high rate of cardiac involvement (60-85%) and 12 genes: *PTPN11*, *SOS1*, *RAF1*, *KRAS*, *HRAS*, *BRAF*, *MEK1/MAP2K1*, *MEK2/MAP2K2*, *NRAS*, *SHOC2*, *CBL* and *SPRED1*. Although the majority of these diseases are readily distinguishable in clinical terms, an integrated imaging study of the cardiac condition associated to *RASopathies* helps to better define risk assessment, surveillance, and management of these patients.

Introduction

RASopathies include a spectrum of disorders due to dysregulation of RAS/mitogen activated protein kinase (MAPK) pathway that plays an essential role in the control of the cell cycle and differentiation. As a consequence, its dysregulation has profound developmental consequences. Although each condition may exhibit unique phenotypic features, many share characteristic overlapping features may occur, including craniofacial dysmorphism, cardiac malformations and cutaneous, musculoskeletal and ocular abnormalities, varying degrees of neurocognitive impairment and, in some syndromes, an increased risk of developing cancer.¹ *RASopathies* (or neurocardiofacio-cutaneous syndromes) with cardiac features are Noonan syndrome, multiple lentiginos syndrome (LEOPARD), cardio-facio-cutaneous (CFC) syndrome, Costello syndrome, neurofibromatosis-1 (NF1), Legius syndrome (NF1-

like), neurofibromatosis-Noonan syndrome (NFNS). The former syndromes are associated with a high rate of cardiac involvement (60-85%) whereas cardiac abnormalities are infrequent in Legius and NF1.

To date, 12 genes are associated with these spectrum of disease: *PTPN11*, *SOS1*, *RAF1*, *KRAS*, *HRAS*, *BRAF*, *MEK1/MAP2K1*, *MEK2/MAP2K2*, *NRAS*, *SHOC2*, *CBL* and *SPRED1* (Table 1).² These gene encode for *Ras proteins*, small guanosine nucleotide-bound GTPases which comprise a critical signaling hub within the cell.³

This high-gene heterogeneity account for variety of phenotypic features, leading to different syndromes. Although the majority of these diseases are readily distinguishable in clinical terms, with or without diagnostic criteria, none of them have any pathognomonic signs. Thus an integrated imaging study of the cardiac condition associated to *RASopathies* helps to better define risk assessment, surveillance, and management of these patients.

RASopathies with cardiac involvement

Noonan syndrome is a well-recognized genetic syndrome with a prevalence of approximately 1 to 3500.^{2,4,5} It is inherited in an autosomal dominant pattern although new cases are common because the de novo mutation rate is high. The common features of Noonan syndrome are short stature, pulmonic stenosis and/or hypertrophic cardiomyopathy, dysmorphic features including hypertelorism, downslanting palpebral fissures, low set posteriorly rotated ears, webbing of the neck and pectus excavatum.² Genitourinary abnormalities are also common, especially cryptorchidism in males, and ophthalmologic problems and sensorineural hearing loss (10%) can occur throughout the lifetime of the affected individual. Developmental delay of variable severity occurs in approximately 25%.^{2,4,6} Patients may also have a coagulopathy and this is important to evaluate and manage appropriately prior to any surgical or invasive procedure.⁷ Finally, there is a threefold increased risk of malignancy in Noonan syndrome: most classically juvenile myelomonocytic leukemia but acute lymphoblastic leukemia, acute myeloid leukemia, rhabdomyosarcoma, and neuroblastoma are seen at higher rates than in the general population as are myeloproliferative disorders.^{2,8-12}

LEOPARD syndrome (LS) [LEOPARD acronyms: lentiginos, electrocardiogram (ECG) abnormalities, ocular hypertelorism, pulmonary stenosis, abnormalities of genitalia, retardation of growth, deafness] is an

Correspondence: Rita Gravino, Corso Umberto I 127, 81050 Santa Maria la Fossa (CE), Italy.
Tel.: +39.338.1996050.
E-mail: ritagravino@virgilio.it

Key words: *RASopathies*, hypertrophic cardiomyopathy, echocardiography.

Conflict of interests: the authors declare no potential conflict of interests.

Received for publication: 17 December 2013.

Revision received: 9 May 2014.

Accepted for publication: 9 May 2014.

This work is licensed under a Creative Commons Attribution NonCommercial 3.0 License (CC BY-NC 3.0).

©Copyright R. Gravino and G. Pacileo, 2014
Licensee PAGEPress, Italy
Cardiogenetics 2014; 4:2198
doi:10.4081/cardiogenetics.2014.2198

autosomal dominant condition whose early diagnosis can be difficult due to phenotypic overlap with Noonan syndrome.² Overlap with the phenotype of NF1 also occurs because both disorders have skin findings of *café-au-lait* macules. Age related development of lentiginos with or without hearing loss was necessary for diagnosis prior to the availability of molecular testing. Approximately 85% of patients have cardiac involvement, with hypertrophic cardiomyopathy (HCM) being most common.¹³ Pulmonary valve stenosis and other structural defects have also been reported. ECG abnormalities are poorly characterized and longitudinal follow-up of a larger cohort is necessary to determine the natural history of cardiac involvement and appropriate surveillance.^{2,14}

Cardio-facio-cutaneous syndrome has substantial overlap with Noonan syndrome but can also be confused with Costello syndrome because of its common ectodermal involvement and more severe intellectual impairment. Skin abnormalities can be extensive and include hyperkeratosis, eczema, palmoplantar hyperkeratosis, and keratosis pilaris. The hair is typically sparse and curly. CFC syndrome has similar cardiac and lymphatic findings to Noonan syndrome.^{2,15} Approximately 75% of patients have cardiac involvement.²

Costello syndrome shares features with Noonan syndrome but is generally regarded as more severe. Unlike Noonan and CFC syndromes that are genetically heterogeneous, Costello syndrome is only caused by *HRAS* mutations that result in constitutive or prolonged activation of the protein.^{2,16} These mutations typically originate from the paternal germline.^{2,17} Facial features in Costello syndrome are coarse. Ectodermal features are

common and include hyperpigmentation, papillomas, and curly hair. In infancy, excessive wrinkling of the skin, especially of the hands and feet, is notable. Individuals with Costello syndrome have an approximately 15% lifetime risk for malignancy. Cardiac involvement includes structural anomalies, HCM, and conduction system abnormalities. Approximately 65-75% of Costello patients with *HRAS* mutations have cardiac involvement.¹⁸⁻²⁰ Pulmonary stenosis occurs in approximately 25%, arrhythmia in 42%, and HCM in 47%. The arrhythmia most commonly described is supraventricular tachycardia, especially chaotic atrial rhythm/multifocal atrial tachycardia, or ectopic atrial tachycardia.²⁰

Neurofibromatosis-1, an autosomal dominant, multisystem disorder that affects approximately one in 3500 individuals, was the first disorder found to originate from a component of the Ras/MAPK pathway.²¹ The NF1 gene product neurofibromin negatively regulates Ras signaling by functioning as a Ras GTPase-activating protein (RasGAP) to accelerate the hydrolysis of active Ras-GTP to inactive Ras-GDP.^{22,23} Loss of neurofibromin leads to hyperactive Ras signaling, as observed by elevated Ras pathway activity in cells.²⁴⁻²⁶ Stowe *et al.* demonstrate that Spred1 down-regulates the Ras/MAPK pathway through an interaction with the NF1 protein neurofibromin.²¹ Importantly, this interaction functions to recruit neurofibromin to the plasma membrane. Furthermore, loss-of-function Spred1 mutants observed in Legius syndrome are either unable to bind neurofibromin or incapable of recruiting it to the membrane. They provide evidence for a molecular link between the phenotypically overlapping developmental disorders Legius syndrome and NF1.²¹ The typical order of appearance of the most common features in NF1 is as follows: *café-au-lait* macules, axillary freckling, Lisch nodules, and neurofibromas. Other features include generalized hyperpigmentation, tumors, skeletal abnormalities, neurologic abnormalities, vasculopathies, and cardiac abnormalities. The increased incidence of heart defects has long been debated.²⁷⁻²⁹

Legius syndrome has been characterized as a milder form of NF1, with individuals displaying multiple *café-au-lait* spots, axillary freckling, and macrocephaly, but lacking other common NF1 manifestations such as Lisch nodules, neurofibromas, osseous lesions, or optic pathway gliomas. Initial experiments revealed that Spred1 mutations were loss-of-function mutations, incapable of inhibiting the Ras/MAPK pathway.³⁰ SPRED1 mutations account for at least 2% of the pathogenic mutations associated with patients clinically diagnosed with NF1.²¹

Neurofibromatosis-Noonan syndrome describes the association of features of Noonan syn-

drome and neurofibromatosis type 1. The genetic origin of these entities is controversial. Most recent reports suggest that NFNS is a variety of NF1 based on the fact that mutations of the *PTPN11* were not found, whereas NF1 gene mutations were the most frequent in these patients. The identification of specific *NFI* alleles recurring in NFNS, the evidence that these alleles co-segregate with the condition in families, and the observation of a peculiar mutational spectrum strongly suggest that the term NFNS does characterize a phenotypic variant of NF1, which manifests with a low incidence of plexiform neurofibromas, skeletal anomalies, and internal tumors, in association with hypertelorism, ptosis, low-set ears, and coronary heart disease (CHDs).³¹

Clinical management, follow-up and treatment of all these conditions greatly overlap. However, a few issues need to be addressed differently, taking into account the specific clinical problems and needs of individuals.

Imaging in the evaluation of cardiac abnormalities detected in RASopathies

An adequate definition of cardiac abnormalities in RASopathies implies a multimaging approach and can be done using different methods which not only allow a diagnosis of each defect, but also define its severity and identify any distinguishing feature. An aim of this review is to define potentials and limits of both standard and new imaging echocardiographic techniques.

Standard transthoracic echocardiogram

Two-dimensional echocardiography (2D-echo) is the most used, cheap and accessible technique in the approach to patients with Rasopathies. Famously, there are cardiac malformations frequently associated with these diseases and their detection can help to define

their clinical diagnosis. The standard echocardiographic approach also helps to characterize these anomalies providing important information about the severity of the clinical situation, prognosis and the most appropriate treatment. Newborns, infants and children suspected of having Rasopathies need a careful cardiac evaluation, including an echocardiogram. Evaluation of the heart in early infancy does not exclude the possibility that an affected child will develop more severe HCM later in childhood. This suggests that serial evaluations during this period are indicated. Cardiac manifestations, most commonly pulmonary valve stenosis and HCM, are present in up to 90% of individuals with Noonan syndrome (NS)^{4,32-34} and, though it is not included in the acronym, HCM is the most frequent anomaly observed in LEOPARD syndrome, representing a potentially life-threatening problem.³⁵ HCM seems to occur with similar frequency in Costello syndrome and LEOPARD syndrome.³⁶

In CFC patients, HCM is identified in 40% of patients and is most frequently diagnosed in infancy but can occur at any age.²

Hypertrophic cardiomyopathy evaluation

In two-dimensional first of all you can evaluate the extent of the maximum wall thickness, the distribution of hypertrophy (Figure 1), the presence of systolic anterior movement (SAM) of the anterior mitral leaflet (AML), the coexistence of right ventricular hypertrophy. To these parameters must be added surely data about the presence of outflow or medioventricular obstruction, left or right.

Wilkinson *et al.* have reported that the NS cohort differs from other children with HCM in many respects.³⁷ They were younger, more likely to have chronic heart failure at diagnosis, more likely to have a family history of genetic syndromes, less likely to have a family

Table 1. Rasopathies with cardiac features: molecular etiologies.

	Noonan	LEOPARD	Costello	Cardio-facio-cutaneous
<i>PTPN11</i>	50%	90%	N/A	N/A
<i>RAF1</i>	3-17%	<5%	N/A	N/A
<i>SOS1</i>	10-20%	N/A	N/A	N/A
<i>KRAS</i>	<5%	N/A	N/A	Rare
<i>NRAS</i>	<1%	N/A	N/A	N/A
<i>BRAF</i>	<2%	<5%	N/A	75%
<i>MAP2K1</i> or <i>MAP2K2</i>	<2%	N/A	N/A	25%
<i>HRAS</i>	-	N/A	80-90%	N/A
<i>SHOC2</i>	<1%	N/A	N/A	N/A

N/A, not available.

history of cardiomyopathy, and had a smaller length/height z score. At diagnosis, left ventricular (LV) fractional shortening (percentage) was higher (52.0 ± 8.9 vs 45.1 ± 8.9 , $P < 0.001$), mean LV mass z score was smaller (mean \pm SD 0.52 ± 2.70 vs 1.87 ± 2.52 , $P < 0.001$), and the median ratio of LV end-diastolic posterior wall thickness to LV end-diastolic dimension was higher (0.32 vs 0.28 , $P = 0.007$) in NS children than in other children with HCM. Asymmetric septal hypertrophy, defined as an end-diastolic septal thickness to LV posterior wall thickness ratio z score ≥ 2 , was noted in 35% of NS compared with 42% of other children with HCM ($P = 0.31$). Left ventricular outflow obstruction was more often present in patients with NS compared with other HCM (30% vs 9%, respectively, $P = 0.01$), but these data were only available for 20 patients with NS. Noting that left-sided lesions (mitral or LV outflow abnormalities) might have affected LV dimension or function during fetal life, they also compared the NS cohort after exclusion of cases with left-sided lesions to the other HCM group. The inferences were similar, implying that the smaller LV size and mass of the NS group is not attributable to the cases of left-sided lesions.

Longitudinal analysis of LV size and function in the NS cohort revealed significant increases in LV end-diastolic and systolic dimension z scores over time (0.25 SD units per year for both, $P < 0.001$) but no change in the LV fractional shortening z score over time. The ratio of LV end-diastolic posterior wall thickness to LV end-diastolic dimension decreased over time (0.013 decrease per year, $P < 0.001$).

In patient with LEOPARD syndrome, HCM, which is generally asymmetric and progressive and commonly involves the intraventricular septum, is detected in up to 80% of the patients with a cardiac defect and may associate with significant left ventricular outflow tract obstruction in up to 40% of the cases.^{13,38-39} Clinical findings of left ventricular hypertrophy are similar to those found in familial HCM.³⁹ However, despite frequent cardiac involvement, most patients are asymptomatic. In relation to left ventricular diastolic function, the most frequent diastolic patterns in patients with left ventricular hypertrophy are abnormal diastolic function, followed closely by abnormal relaxation and more rarely by a restrictive filling pattern.³⁸

In infants and very young child, Costello syndrome can overlap Noonan syndrome. Both can present with HCM of variable severity, including severe infantile HCM.^{13,40,41} In approximately one-third of Costello syndrome patients each, in fact, HCM was be chronically severe or worsen during follow-up. The resolution or regression of HCM was reported in one patient with a KRAS mutation.⁴²

Anecdotal experience suggests that severe

subaortic obstruction requiring surgical treatment is more frequent in Costello syndrome than in Noonan or CFC. The resolution by echocardiographic criteria of HCM in five patients with Costello syndrome is not unique among RASopathies, and requires monitoring across the spectrum of RASopathies in longitudinal studies.³⁶

Compared to children with hypertrophic cardiomyopathy, those with left ventricular hypertrophy in the setting of Noonan or LEOPARD syndromes show more severe diastolic dysfunction, due to both abnormal relaxation and reduced compliance. They also exhibit an increased prevalence of obstruction of the left ventricular outflow tract, along with dynamic obstruction of the right ventricular outflow tract.⁴³

Coronary heart diseases evaluation

Among the RASopathies, CHDs appear most common (~90% of patients with a cardiac problem).³⁶ Congenital heart defects are present in 85% of Noonan syndrome patients, in whom the most prevalent cardiac anomaly is pulmonary valve stenosis (Figure 2), with an incidence of 50% to 60%.²

The valve may be dysplastic in 25% to 35%⁽⁴⁴⁻⁴⁶⁾ of them and is often associated with an atrial septal defect. The anatomic pattern is quite distinct, with dysplastic pulmonary valve and fibrous thickening of the anulus and the leaflets. Stenosis results from fibrous thickening of the valvular leaflets which appear deformed, glistening and edematous, eventually without fusion of commissures.⁴⁷ Pulmonary valve insufficiency and right ventricular dysfunction are potential problems after earlier pulmonary valve surgery so they can be detected in these patients. Pulmonary stenosis is less frequent than left ventricular hypertrophy in patients with LS. Limongelli *et al.*³⁹ observed pulmonary stenosis in 23% of the patients with LS (valvular, isolated infundibular, valvular and infundibular or

with a dysplastic pulmonary valve). Pulmonary stenosis in Costello syndrome, usually valvar, is common, and may include muscular subpulmonary obstruction (related to HCM), as well as supravalvar narrowing. Rare patients with severe subpulmonary stenosis described as *double-chambered right ventricle* may have accounted for early reports of *biventricular* cardiomyopathy.³⁶ Pulmonary valve stenosis have been also identified in 25% of patients with CFC.²

Other common structural defects in NS include branch pulmonary artery stenosis, septal defects, especially secundum atrial septal defects and partial atrioventricular canal defects, and tetralogy of Fallot. Although coarctation of the aorta was originally thought to be a differentiating feature between Noonan and Turner syndromes, more recent data indicate that aortic coarctation is not rare in Noonan syndrome. In addition, cardiac abnormalities include an over-representation of mitral valve dysplasia and septal defects.² Structural abnormalities of mitral valve have been observed in patients with NS and LS alone or in association with HCM. An isolated anomalous insertion of mitral valve on the ventricular septum causing obstruction of the left ventricular outflow tract has been rarely observed in these patients. The leaflets of mitral valve can be dysplastic with short cords and nodular mixomatous tissue.⁴⁸

Abnormalities of the aortic valve (23%; *e.g.* mild aortic regurgitation, discrete subaortic stenosis or aortic valve dysplasia) and mitral valve (38%; *e.g.* mitral valve prolapse) result more frequent in LS.² Atrial septal defects, ventricular septal defects, mitral or tricuspid valve dysplasia and bicuspid aortic valve are all identified with lesser frequency in CFC.²

In patients with Costello syndrome, then, in addition to pulmonary valve stenosis or dysplasia, anomalies of the other valves were seen, including thick aortic valve, mitral valve prolapse without HCM, and in some cases polyval-

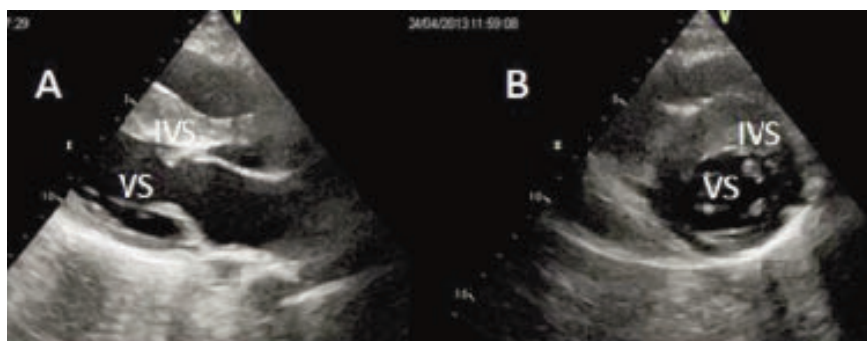


Figure 1. Two-dimensional echocardiographic image of hypertrophic cardiomyopathy in a patient with Costello syndrome with evidence in the long axis (A) and short axis (B) views of a severe asymmetric hypertrophy of the left ventricle (LV), mainly localized at the level of the interventricular septum (IVS).

var dysplasia (mitral/tricuspid valve prolapse; thick mitral/aortic valve and dysplasia of all 4 valves; mitral valve prolapse/bicuspid aortic valve). Valve anomalies can be associated with various minor CHDs including muscular ventricular septal defect and thick aortic valve, and atrial septal defect with bicuspid aortic valve. Septal defects were usually hemodynamically insignificant, including ventricular septal defect, type unspecified, isolated atrial septal defect, atrial septal defect with pulmonary stenosis, and combinations (with coarctation, ventricular septal defect, atrial septal defect; membranous ventricular septal defect, transient polyvalvular disease).³⁶

In NF1, the abnormalities (2.1%) included atrial septal defects, atrial septal aneurysms, pulmonary stenosis, coarctation of the aorta, mitral valve prolapse, mitral regurgitation, aortic regurgitation, and hypertrophic cardiomyopathy⁴⁹ and, in Legius syndrome patients, examples of findings reported in isolated or only a few individuals include pulmonic stenosis and mitral valve prolapsed.

Furthermore, coronary abnormalities, such as dilatation of the coronary arteries, abnormalities of the left ventricular shape, segmental wall motion, apical aneurysm of the left ventricle, non-compacted left ventricle, isolated left ventricular enlargement, atrioventricular septal defects and ventricular septal defects were found in RASopathies.³⁵ Aortic dilation has been rarely reported in patients with Noonan syndrome. Coronary artery dilation and peripheral aneurysms have been reported LS,^{13,50,51} with aortic dilation in one clinically diagnosed patient.⁵²

New imaging techniques. Although not yet reported experience in the literature about the use of these techniques in the study of patients with rasopathies, the wide range of information derived from the analysis of non-syndromic heart disease or those associated with other syndromes leads us to predict their routine use in all patients.⁵³

The evolution of newer ultrasound-based technologies such as tissue Doppler imaging (TDI), strain imaging, speckle tracking-based LV torsion analysis, and three-dimensional echocardiography (3D-echo) has revolutionized the assessment of cardiac performance from mere assessment of ejection fraction to a more sophisticated appraisal of regional cardiac mechanics.⁵⁴⁻⁵⁷ The complex deformations that constitute systolic contraction, including: ventricular twist; longitudinal, circumferential, and radial displacement; velocities; strain; and strain rate can now be reliably quantified.⁵⁸⁻⁶³ These may be useful techniques in the cardiac evaluation of RAS/MAPK syndromes but further studies will need to evaluate this aspect. These novel technologies have provided profound mechanistic insight into abnormalities of regional contractility and

diastolic function and have enabled the non-invasive characterization of abnormal intramural myocardial mechanics emblematic of HCM, for example. In addition, these advances have facilitated pre-clinical diagnosis,^{64,65} refined risk stratification,^{66,67} and furthered our understanding of existing therapies for HCM.^{68,69,70}

In addition, new echocardiographic techniques can be of great help in improving the evaluation and study of congenital heart disease.

Tissue Doppler imaging

Tissue Doppler and deformation imaging, including Doppler-derived strain and speckle tracking, have significantly improved our understanding of cardiac mechanics in both physiological and pathological states.^{54,71,72} The various modes of left ventricular deformation (longitudinal, circumferential, radial and twist) leading to systolic contraction can nowadays be quantified.^{54,71,72} One of the best applications of deformation imaging is in the area of hypertrophic cardiomyopathies.^{53,73,74}

Systolic myocardial velocity, a measure of longitudinal systolic function, has been shown to be attenuated in HCM (Figure 3), even in nonhypertrophied ventricular segments.⁷⁵ Early diastolic mitral annular velocity is a pre-load-independent index for evaluating diastolic function. Early mitral annular velocities are reduced in patients with HCM compared with age-matched controls and relate to the magnitude of ventricular hypertrophy.⁷⁶ Useful diagnostic^{64,77,78} as well prognostic⁷⁹ information has emerged from clinical studies assessing the role of TDI in patients with HCM. First,

Nagueh *et al.*⁶⁴ investigated myocardial velocities in genotype-positive individuals with HCM in the absence or presence of left ventricular hypertrophy (LVH). Compared with normal controls, all individuals with HCM presented significantly reduced systolic tissue velocities (Sa) and early diastolic tissue velocities at both corners of the mitral annulus. The use of TDI also can assist in differentiating between variants of LVH. Vinereanu *et al.*⁵⁷ used TDI to distinguish pathological from physiological LVH in a study comprising patients with HCM, patients with systemic hypertension, athletes, and normal subjects. A significant negative correlation also has been observed between TDI Sa (peak systolic), early diastolic mitral annular velocities, and left ventricular outflow tract (LVOT) peak gradient, underscoring the influence of LVOT obstruction on longitudinal myocardial performance.⁷⁹ In a recent report of patients with established HCM, low lateral mitral annular systolic velocity (<4 cm/s) was found to have prognostic value and independently predicted death or hospitalization for worsening heart failure.⁸⁰

Although TDI was initially advocated as a technique for assessing regional myocardial performance, its inability to discern myocardial contractility from passive motion led to the development of strain imaging that assesses myocardial motion relative to the adjacent myocardium.⁵⁸ Systolic myocardial strain (ϵ) is a dimension-less quantity and a measure of tissue deformation. TDI-derived strain was first used for the evaluation of HCM by Weidemann *et al.*⁸¹ in a case report of a child with non-obstructive HCM. Subsequently, Yang

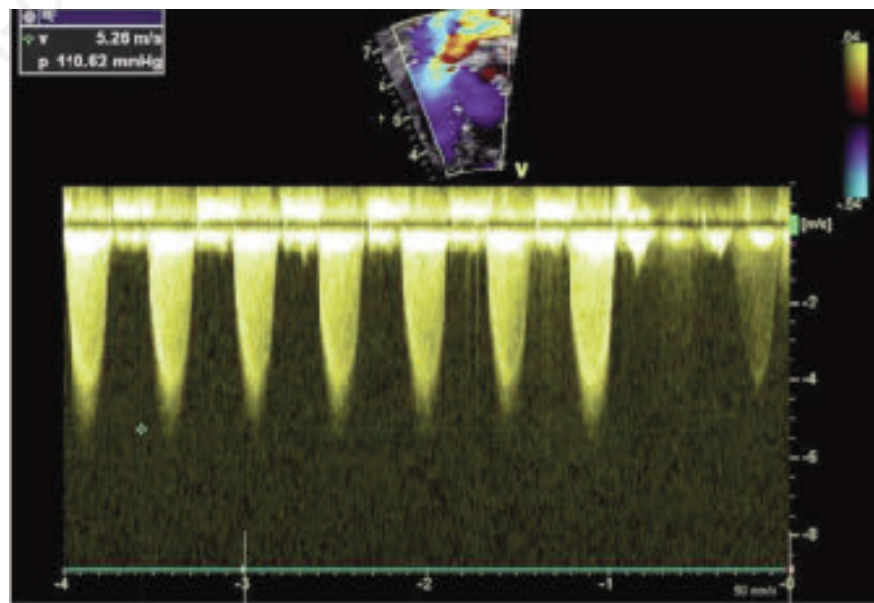


Figure 2. Doppler study of severe pulmonary valve stenosis in a patient with Noonan syndrome.

*et al.*⁸² reported the assessment of regional myocardial function in 31 adults with HCM diagnosed echocardiographically. This study, along with the case reported by Weidemann *et al.*,⁸¹ highlight the relevance of myocardial disarray and fibrosis on regional performance (rapidly and reproducibly detected by strain imaging), because the commonly affected mid-septum typically shows the greatest degree of dysfunction. Longitudinal deformation abnormalities in HCM often are focal or subsegmental and may be underestimated when conventional segmental techniques are used to estimate myocardial strain. Sengupta *et al.*⁸³ compared ϵ values using a conventional technique to linear mapping in 20 healthy volunteers and 20 individuals with HCM. These data suggest that the heterogeneity of myocardial function in HCM ranges from focal subsegmental to larger segmental abnormalities and emphasize the need for careful spatial mapping to increase diagnostic yield. This effort can be facilitated by information gleaned from parametric color strain maps.

Speckle tracking imaging

This rapidly expanding technology entails spatial and temporal tracking of adjacent naturally occurring acoustic markers or *speckles* from standard black and white echocardiographic images in 2 dimensions (Figure 4). Interestingly, a base-apex gradient was described, with a progressive increase in longitudinal strain values noted from basal to apical segments. Serri *et al.*⁶³ applied 2D strain echocardiography to a subset of patients with familial non-obstructive HCM. Average longitudinal ϵ was reduced in affected individuals compared with healthy controls ($15.1 \pm 6.2\%$ vs $20.3 \pm 5.6\%$), despite apparently normal systolic function (with the use of standard criteria). No significant difference in the values obtained by TDI versus 2D ϵ was observed. Furthermore, transverse, circumferential, and radial strain were significantly reduced in affected individuals ($23.3 \pm 17\%$ vs $27.2 \pm 14.9\%$, $16.8 \pm 7.1\%$ vs $19.6 \pm 5.2\%$, $25.2 \pm 13.9\%$ vs $36.8 \pm 17.2\%$, respectively). Although overall longitudinal values were reduced in the HCM group, a base to apex gradient was still observed, as in the control group. Similarly, radial strain in the mid- and apical short-axis segments in HCM was significantly attenuated compared with patients with hypertensive LVH.⁶⁷ The authors concluded that 2D ϵ can be used to identify subclinical global systolic dysfunction in patients with HCM, with improved interobserver as well as intraobserver variability compared with TDI-derived strain (7.5% vs 13.7% and 7.9% vs 14.5% , respectively).

Because of its intrinsic ability to provide angle-independent strain data, 2D strain holds a unique advantage over tissue Doppler-derived strain, which is particularly relevant

when one analyzes myocardial deformation in the apical LV segments.

Left ventricular twist is defined as the difference between the mean values on the peak rotation at the apical and at the mitral valve level (twist $\frac{1}{4}$ mean peak apical rotation $\times 2$ mean peak basal rotation).

Similarly LV twist rate is defined as the difference between the mean values of the peak

rotation rate at the apical and at the mitral valve level (twist rate $\frac{1}{4}$ mean peak apical rotation rate $\times 2$ mean peak basal rotation rate). The untwisting onset is expressed as a percentage of systolic duration (the ratio between the time to peak twist, *i.e.* onset of untwisting, and the duration of systole until the aortic valve closure) by the use of cardiac cycles with matched RR intervals (time to peak twist/sys-

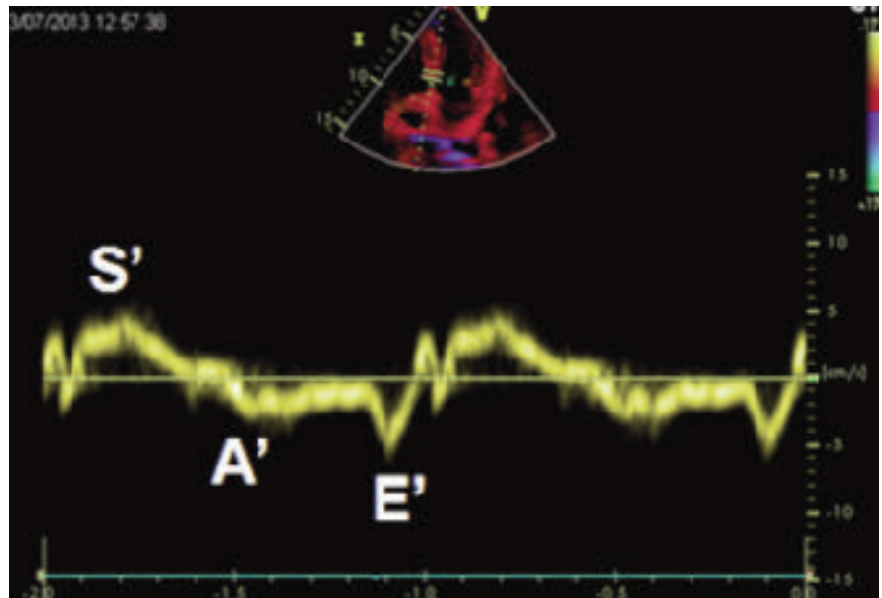


Figure 3. Reduced systolic velocity (S') and altered diastolic patterns (inverted ratio A'/E') at the level of the basal segment of the interventricular septum in patients with hypertrophic cardiomyopathy.

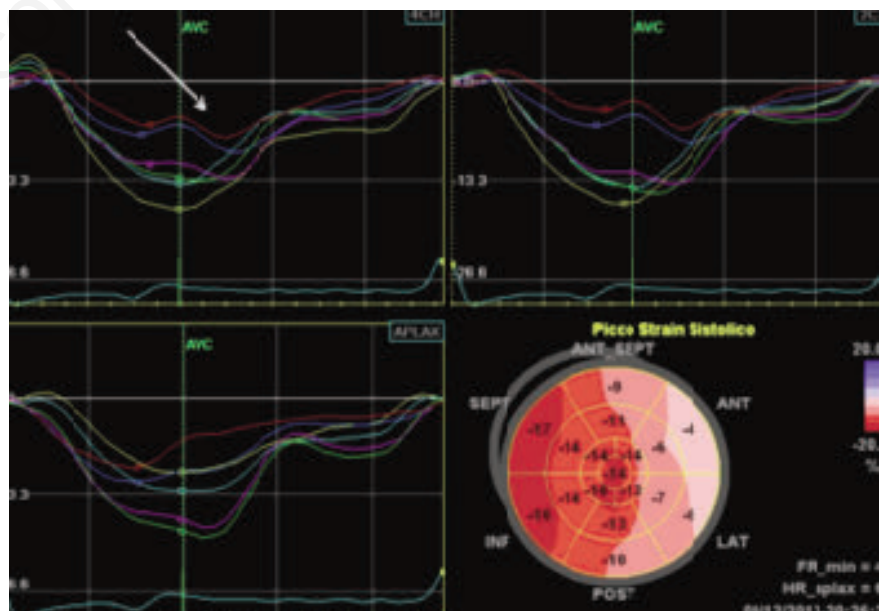


Figure 4. Two-dimensional strain study in a patient with hypertrophic cardiomyopathy: reduced peak of strain of the hypertrophic segments evidenced in the corresponding curve (arrow) and reduced segmental myocardial deformation evidenced in the schematic bull eye.

toxic time). This normalization for systolic duration has to be made to overcome the heart rate dependence, as previously described.

All CM patients have an impairment of the longitudinal, circumferential, and radial myocardial deformations. Peak LV twist is preserved in patients with normal or increased ejection fraction (EF). However, LV twist is prolonged and untwisting is delayed in all CM patients (even with normal EF and peak systolic twist), suggesting that a mechanical adaptation to subclinical systolic abnormalities might induce, by a prolonged LV twist, the onset of an early diastolic dysfunction.⁸⁴

The usefulness of these new technologies is further confirmed in the study of congenital heart disease.^{85,86} Also in this case the experiences reported in the literature do not relate specifically to patients suffering from rasopathies but, undoubtedly, the collected data open new openings of application also in this type of patients.

Speckle tracking imaging can be useful for the study of right ventricle in congenital heart disease too.

Patients with tetralogy of Fallot undergoing surgical correction, even if asymptomatic, showed an alteration of the properties of longitudinal strain of the right ventricle considering strain and strain rate, and these changes are accentuated in patients in which it was carried out the reconstruction of the outflow tract of the right ventricle compared to correction by infundibular patch.⁸⁷ Another study showed that the two-dimensional longitudinal strain and strain rate were reduced 1 month after the surgical replacement of the pulmonary valve, then after 6 months had increased although without reaching the pre-intervention values.⁸⁸ A longer follow-up may show whether the right ventricular dysfunction after pulmonary valve replacement is stable or transient, but in conclusion we can say that beyond the clinical and hemodynamic improvement has questioned the actual improvement of right ventricular function after surgical correction.

Three-dimensional echocardiography

The use of 3D-echo has provided insights into the mechanics of SAM and deformational geometry of the LV outflow tract.⁸⁹ Data suggest that the medial segments of the mitral valve are predominantly involved in SAM, resulting in a narrow laterally located LVOT in patients with obstructive cardiomyopathy.⁹⁰ Likewise, 3D-echo facilitates the assessment of LVOT area after intervention for septal reduction,⁹¹ and after surgical myectomy,⁹² volumetric estimates of left atrial mechanical function,⁹³ and accurate estimation of LV ejection fraction as well as LV mass in hypertrophied hearts (comparing favorably with cardiac magnetic resonance imaging).⁹⁴ Live 3D-echo also improves recognition of location and extent of LV cavity

obliteration⁹⁵ and may be used in conjunction with LV contrast opacification for this purpose.⁹⁶ Echocardiographic evaluation of pulmonary valve (PV) anatomy is more difficult than other valves due to poor acoustic access even by 2D-transsthoracic echocardiogram (TTE).⁹⁷ Real-time (RT)3D-TTE could describe the morphological features of the 3 cusps simultaneously through the en face view only in 60% of patients.⁹⁸ This percentage increases in patients with pulmonary stenosis due to increased cusp thickness.⁹⁹ In study, only 5 patients with PV stenosis were examined by RT3D-TTE. It was possible to assess the cusp thickness, commissures and mobility in addition to measurement of PV annulus (area and diameter) and PV area.

The 3D study of the right ventricle in pediatric cardiology seems particularly promising since the frequent involvement of this chamber of the heart in congenital heart disease. It is also well established that in pressure overload of the right ventricle congenital classic numerical systolic function do not correlate with cardiac function in these patients the radial function prevails and overcomes the longitudinal, therefore may be useful other indices such as ejection fraction or the three-dimensional transverse strain.

Finally has been demonstrated in some studies a correlation between volumes and function of a functionally single ventricle (right or left) calculated through resonance and echo 3D.

Currently there are new probes pediatric transthoracic three-dimensional high-frequency three-dimensional image that improve the quality and allow you to use this method in children. Also, the ability today to have a three-dimensional view image directly using special glasses increases the immediacy of the technique. There is some evidence on the usefulness Three-dimensional imaging in selected patients with congenital heart disease, but the extensive use of echocardiography laboratories for congenital heart disease remains to be determined.

Significant technical limitation for application in pediatric full volume is the acquisition that requires breath holding and sometimes sedation (child). On the other hand for all congenital heart disease need a custom post-processing, which consists in aligning the image with the anatomical structure to be studied in the best point of view, the post-processing can be long and tedious and requires an appropriate learning curve.

Magnetic resonance imaging

Magnetic resonance imaging (MRI) is an important imaging technique with an expanding role in the contemporary evaluation of patients with HCM; it provides complete LV reconstruction and a precise definition of the

distribution and pattern of hypertrophy. This is particularly useful in patients without a clear LV anatomic characterization by echocardiography. Measurements of maximum wall thickness (MWT) by echocardiography and by MRI are strictly related whereas MWT shows weak relationship when related to LV mass.

In patients highly suspected to have HCM, but with a negative echocardiogram for LV hypertrophy, MRI represents an additive diagnostic chance as proposed by Rickers *et al.* Authors found, in a population involving almost 50 patients, that MRI was capable of identifying regions of LV hypertrophy (in particular at anterolateral level) not readily recognized by echocardiography, which were solely responsible for diagnosis of the HCM phenotype in an important minority of patients.¹⁰⁰ Moreover, the measure of LV mass and the characterization of abnormal substrate of fibrosis will probably provide implications of these findings in the risk stratification.¹⁰¹⁻¹⁰⁷ Nevertheless, it must be underscored that MRI doesn't provide complete LV tissue characterization and, thus, can not be used as a non-invasive biopsy.

In patients with valvular heart disease, MRI is uniquely suited to identify and assess the magnitude of valvular stenosis or regurgitation, as well as determine the influence of the valve lesion on ventricle performance. The subjective presence or absence of valvular disease can be made on cine GRE sequences by visualization of a signal void/turbulent jet above or below the valve in systole or diastole.

MRI imaging can be used to assess the pulmonary arteries for pulmonary arterial stenoses (as in congenital heart disease). Pulmonary arterial size can also be assessed. Primarily, pulmonary contrast enhancement magnetic resonance angiography (CE-MRA) is used with the bolus timed to opacify the pulmonary arteries at the center of k-space data acquisition.

Time-resolved CE-MRA is particularly useful for imaging the pulmonary vasculature as it allows complete separation of the pulmonary and systemic phases.

MRI may be used for identifying coronary artery anomalies and aneurysms and for determining coronary artery patency. In specialized centers, MRI may be uniquely useful in identifying coronary artery disease without exposure to ionizing radiation or iodinated contrast medium.¹⁰⁸

Conclusions

All imaging techniques provide important and useful information on the most frequent cardiac abnormalities observed in the RASopathies. The use of recent imaging meth-

ods requires, though, specific expertise. The identification of specific defects (HCM, PVS, CHDs), which represent *hallmarks* of these syndromes, requires careful clinical evaluation and specific management and treatment.

References

1. Tidyman WE, Rauen KA. The RASopathies: developmental syndromes of Ras/MAPK pathway dysregulation. *Curr Opin Genet Dev* 2009;19:230-6.
2. Ware SM, Jefferies JL. New genetic insights into congenital heart disease. *J Clin Exp Cardiol* 2012;S8:pil:003.
3. Yoon S, Seger R. The extracellular signal-regulated kinase: multiple substrates regulate diverse cellular functions. *Growth Factors* 2006;24:21-44.
4. Romano AA, Allanson JE, Dahlgren J, et al. Noonan syndrome: clinical features, diagnosis, and management guidelines. *Pediatrics* 2010;126:746-59.
5. Noonan JA. Hypertelorism with Turner phenotype. A new syndrome with associated congenital heart disease. *Am J Dis Child* 1968;116:373-80.
6. Lee DA, Portnoy S, Hill P, et al. Psychological profile of children with Noonan syndrome. *Dev Med Child Neurol* 2005;47:35-8.
7. Derbent M, Oncel Y, Tokel K, et al. Clinical and hematologic findings in Noonan syndrome patients with PTPN11 gene mutations. *Am J Med Genet A* 2010;152A:2768-74.
8. Tartaglia M, Martinelli S, Stella L, et al. Diversity and functional consequences of germline and somatic PTPN11 mutations in human disease. *Am J Hum Genet* 2006;78:279-90.
9. Denayer E, Devriendt K, de Ravel T, et al. Tumor spectrum in children with Noonan syndrome and SOS1 or RAF1 mutations. *Genes Chromosomes Cancer* 2010;49:242-52.
10. Jongmans MC, Hoogerbrugge PM, Hilkens L, et al. Noonan syndrome, the SOS1 gene and embryonal rhabdomyosarcoma. *Genes Chromosomes Cancer* 2010;49:35-64.
11. Jongmans MC, van der Burgt I, Hoogerbrugge PM, et al. Cancer risk in patients with Noonan syndrome carrying a PTPN11 mutation. *Eur J Hum Genet* 2011;19:870-4.
12. Kratz CP, Niemeyer CM, Castleberry RP, et al. The mutational spectrum of PTPN11 in juvenile myelomonocytic leukemia and Noonan syndrome/myeloproliferative disease. *Blood* 2005;106:2183-5.
13. Limongelli G, Pacileo G, Matino B, et al. Prevalence and clinical significance of cardiovascular abnormalities in patients with the LEOPARD syndrome. *Am J Cardiol* 2007;100:736-41.
14. Limongelli G, Sarkozy A, Pacileo G, et al. Genotype-phenotype analysis and natural history of left ventricular hypertrophy in LEOPARD syndrome. *Am J Med Genet A* 2008;146A:620-8.
15. Roberts A, Allanson J, Jadico SK, et al. The cardiofaciocutaneous syndrome. *J Med Genet* 2006;43:833-42.
16. Aoki Y, Niihori T, Kawame H, et al. Germline mutations in HRAS proto-oncogene cause Costello syndrome. *Nat Genet* 2005;37:1038-40.
17. Sol-Church K, Stabley DL, Nicholson L, et al. Paternal bias in parental origin of HRAS mutations in Costello syndrome. *Hum Mutat* 2006;27:736-41.
18. Rauen KA, Schoyer L, McCormick F, et al. Proceedings from the 2009 genetic syndromes of the Ras/MAPK pathway: From bedside to bench and back. *Am J Med Genet A* 2010;152A:4-24.
19. Gripp KW, Lin AE, Stabley DL, et al. HRAS mutation analysis in Costello syndrome: genotype and phenotype correlation. *Am J Med Genet A* 2006;140:1-7.
20. Lin AE, Grossfeld PD, Hamilton RM, et al. Further delineation of cardiac abnormalities in Costello syndrome. *Am J Med Genet* 2002;111:115-29.
21. Stowe IB, Mercado EL, Stowe TR, et al. A shared molecular mechanism underlies the human rasopathies Legius syndrome and Neurofibromatosis-1. *Genes Dev* 2012;26:1421-6.
22. Martin GA, Viskochil D, Bollag G, et al. The GAP-related domain of the neurofibromatosis type 1 gene product interacts with ras p21. *Cell* 1990;63:843-9.
23. Xu GF, O'Connell P, Viskochil D, et al. The neurofibromatosis type 1 gene encodes a protein related to GAP. *Cell* 1990;62:599-608.
24. Basu TN, Gutmann DH, Fletcher JA, et al. Aberrant regulation of ras proteins in malignant tumour cells from type 1 neurofibromatosis patients. *Nature* 1992;356:713-5.
25. De Clue JE, Papageorge AG, Fletcher JA, et al. Abnormal regulation of mammalian p21ras contributes to malignant tumor growth in von Recklinghausen (type 1) neurofibromatosis. *Cell* 1992;69:265-73.
26. Bollag G, Clapp DW, Shih S, et al. Loss of NF1 results in activation of the Ras signaling pathway and leads to aberrant growth in haematopoietic cells. *Nat Genet* 1996;12:144-8.
27. Oderich GS, Sullivan TM, Bower TC, et al. Vascular abnormalities in patients with neurofibromatosis syndrome type I: clinical spectrum, management, and results. *J Vasc Surg* 2007;46:475-84.
28. Lin AE, Garver KL. Cardiac abnormalities in neurofibromatosis. *Neurofibromatosis*. 1988;1:146-51.
29. Tedesco MA, Di Salvo G, Natale F, et al. The heart in neurofibromatosis type I: an echocardiographic study. *Am Heart J* 2002;143:883-8.
30. Brems H, Chmara M, Sahbatou M, et al. Germline loss-of-function mutations in SPRED1 cause a neurofibromatosis 1-like phenotype. *Nat Genet* 2007;39:1120-6.
31. De Luca A, Bottillo I, Sarkozy A, et al. NF1 gene mutations represent the major molecular event underlying neurofibromatosis-Noonan syndrome. *Am J Hum Genet* 2005;77:1092-101.
32. Kaski JD, Syrris P, Shaw A, et al. Prevalence of sequence variants in the RAS-mitogen activated protein kinase signaling pathway in pre-adolescent children with hypertrophic cardiomyopathy. *Circ Cardiovasc Genet* 2012;5:317-26.
33. Tartaglia M, Zampino G, Gelb BD. Noonan syndrome: clinical aspects and molecular pathogenesis. *Mol Syndromol* 2010;1:2-26.
34. Sharland M, Burch M, McKenna WM, et al. A clinical study of noonan syndrome. *Arch Dis Child* 1992;67:178-83.
35. Martínez-Quintana E, Rodríguez-González F. LEOPARD syndrome: clinical features and gene mutations. *Mol Syndromol* 2012;3:145-57.
36. Lin AE, Alexander ME, Colan SD, et al. Clinical, pathological, and molecular analyses of cardiovascular abnormalities in Costello syndrome: a Ras/MAPK pathway syndrome. *Am J Med Genet Part A* 155:486-507.
37. Wilkinson JD, Lowe AM, Salbert BA, et al. Outcomes in children with Noonan syndrome and hypertrophic cardiomyopathy: a study from the Pediatric Cardiomyopathy Registry. *Am Heart J* 2012;164:442-8.
38. Martínez-Quintana E, Rodríguez-González F. LEOPARD syndrome and hypertrophic cardiomyopathy. *Radiologia* 2011;53:284-6.
39. Limongelli G, Hawkes L, Calabrò R et al. Mutation screening of the PTPN11 gene in hypertrophic cardiomyopathy. *Eur J Med Genet* 2006;49:426-30.
40. Hinek A, Teitel MA, Schoyer L, et al. Myocardial storage of chondroitin sulfate-containing moieties in Costello syndrome patients with severe hypertrophic cardiomyopathy. *Am J Med Genet Part A* 2005;133A:1-12.
41. Lo IFM, Brewer C, Shannon N, et al. Severe neonatal manifestations of Costello syndrome. *J Med Genet* 2009;45:167-71.
42. Sovik O, Schubert S, Houge G, et al. De novo HRAS and KRAS mutations in two

- sib-lings with short stature and neuro-cardio-facio-cutaneous features. *J Med Genet* 2007;44:e84.
43. Cerrato F, Pacileo G, Limongelli G et al. A standard echocardiographic and tissue Doppler study of morphological and functional findings in children with hypertrophic cardiomyopathy compared to those with left ventricular hypertrophy in the setting of Noonan and LEOPARD syndromes. *Cardiol Young* 2008;18:575-80.
 44. Sznajder Y, Keren B, Baumann C, et al. The spectrum of cardiac anomalies in Noonan syndrome as a result of mutations in the PTPN11 gene. *Pediatrics* 2007;119:e1325-31.
 45. Burch M, Sharland M, Shinebourne E, et al. Cardiologic abnormalities in Noonan syndrome: phenotypic diagnosis and echocardiographic assessment of 118 patients. *J Am Coll Cardiol* 1993;22:1189-92.
 46. Ishizawa A, Oho S, Dodo H, et al. Cardiovascular abnormalities in Noonan syndrome: the clinical findings and treatments. *Acta Paediatr Jpn* 1996;38:84-90.
 47. Marino B, Digilio MC, Toscano A, et al. Congenital heart diseases in children with Noonan syndrome: an expanded cardiac spectrum with high prevalence of atrioventricular canal. *J Pediatr* 1999; 135:703-6.
 48. Marino B, Gagliardi MG, Digilio MC, et al. Noonan syndrome: structural abnormalities of the mitral valve causing subaortic obstruction. *Eur J Pediatr* 1995;154:949-52.
 49. Fox CJ, Tomajian S, Kaye AJ, et al. Perioperative management of neurofibromatosis. Type 1. *Ochsner J* 2012;12:111-21.
 50. Yagubyan M, Panneton JM, Lindor NM, et al. LEOPARD syndrome: a new polyaneurysm association and an update on the molecular genetics of the disease. *J Vasc Surg* 2004;39:897-900.
 51. Iwasaki Y, Horigome H, Takahashi-Igari M, et al. Coronary artery dilatation in LEOPARD syndrome. A child case and literature review. *Congenit Heart Dis* 2009; 4:38-41.
 52. Goyal SB, Aragam JR. Aortic root dilatation with redundancy of mitral and aortic leaflets associated with the LEOPARD syndrome. *Int J Cardiol* 2006;110:110-11.
 53. Afonso LC, Bernal J, Bax JJ, et al. Echocardiography in hypertrophic cardiomyopathy: the role of conventional and emerging technologies. *JACC Cardiovasc Imaging* 2008;1:787-800.
 54. Sutherland GR, Di Salvo G, Claus P, et al. Strain and strain rate imaging: a new clinical approach to quantifying regional myocardial function. *J Am Soc Echocardiogr* 2004;17:788-802.
 55. Helle-Valle T, Crosby J, Edvardsen T, et al. New noninvasive method for assessment of left ventricular rotation: speckle tracking echocardiography. *Circulation* 2005; 112:3149-56.
 56. Ho CY, Solomon SD. A clinician's guide to tissue Doppler imaging. *Circulation* 2006;113:e396-8.
 57. Vinereanu D, Florescu Net, Sculthorpe N, et al. Differentiation between pathologic and physiologic left ventricular hypertrophy by tissue Doppler assessment of long-axis function in patients with hypertrophic cardiomyopathy or systemic hypertension and in athletes. *Am J Cardiol* 2001;88:53-8.
 58. Marwick TH. Measurement of strain and strain rate by echocardiography: ready for prime time? *J Am Coll Cardiol* 2006;47: 1313-27.
 59. Perk G, Tunick PA, Kronzon I. Non-Doppler two-dimensional strain imaging by echo-cardiography - from technical considerations to clinical applications. *J Am Soc Echocardiogr* 2007;20:234-43.
 60. Yip G, Abraham T, Belohlavek M, et al. Clinical applications of strain rate imaging. *J Am Soc Echocardiogr* 2003;16: 1334-42.
 61. Notomi Y, Martin-Miklovic MG, Oryszak SJ, et al. Enhanced ventricular untwisting during exercise: a mechanistic manifestation of elastic recoil described by Doppler tissue imaging. *Circulation* 2006;113:2524-33.
 62. Notomi Y, Lysyansky P, Setser RM, et al. Measurement of ventricular torsion by two-dimensional ultrasound speckle tracking imaging. *J Am Coll Cardiol* 2005;45:2034-41.
 63. Serri K, Reant P, Lafitte M, et al. Global and regional myocardial function quantification by two-dimensional strain: application in hypertrophic cardiomyopathy. *J Am Coll Cardiol* 2006;47:1175-81.
 64. Nagueh SF, Bachinski LL, Mayer D, et al. Tissue Doppler imaging consistently detects myocardial abnormalities in patients with hypertrophic cardiomyopathy and provides a novel means for an early diagnosis before and independently of hypertrophy. *Circulation* 2001;104:128-30.
 65. Nagueh SF, McFalls J, Mayer D, et al. Tissue Doppler imaging predicts the development of hypertrophic cardiomyopathy in subjects with subclinical disease. *Circulation* 2003;108:395-8.
 66. D'Andrea A, Caso P, Severino S, et al. Prognostic value of intra left ventricular electromechanical asynchrony in patients with hypertrophic cardiomyopathy. *Eur Heart J* 2006;27:1311-8.
 67. D'Andrea A, Caso P, Severino S, et al. Association between intraventricular myocardial systolic dyssynchrony and ventricular arrhythmias in patients with hypertrophic cardiomyopathy. *Echocardiography* 2005;22:571-8.
 68. Nagakura T, Takeuchi M, Yoshitani H, et al. Hypertrophic cardiomyopathy is associated with more severe left ventricular dyssynchrony than is hypertensive left ventricular hypertrophy. *Echocardiography* 2007;24:677-84.
 69. Carasso S, Woo A, Yang H, et al. Myocardial mechanics explains the time course of benefit for septal ethanol ablation for hypertrophic cardiomyopathy. *J Am Soc Echocardiogr* 2008;21:493-9.
 70. Abraham TP, Nishimura RA, Holmes DR Jr, et al. Strain rate imaging for assessment of regional myocardial function: results from a clinical model of septal ablation. *Circulation* 2002;105:1403-6.
 71. Gorcsan J 3rd, Tanaka H. Echocardiographic assessment of myocardial strain. *J Am Coll Cardiol* 2011; 58:1401-13.
 72. Mor-Avi V, Lang RM, Badano LP, et al. Current and evolving echocardiographic techniques for the quantitative evaluation of cardiac mechanics: ASE/EAE consensus statement on methodology and indications endorsed by the Japanese Society of Echocardiography. *Eur J Echocardiogr* 2011;12:167-205.
 73. Cikes M, Sutherland GR, Anderson LJ, et al. The role of echocardiographic deformation imaging in hypertrophic myopathies. *Nat Rev Cardiol* 2010;7:384-96.
 74. Di Salvo G, Pacileo G, Limongelli G, et al. Non sustained ventricular tachycardia in hypertrophic cardiomyopathy and new ultrasonic derived parameters. *J Am Soc Echocardiogr* 2010;23:581-90.
 75. Cardim N, Oliveira AG, Longo S, et al. Doppler tissue imaging: regional myocardial function in hypertrophic cardiomyopathy and in athlete's heart. *J Am Soc Echocardiogr* 2003;16:223-32.
 76. Matsumura Y, Elliott PM, Virdee MS, et al. Left ventricular diastolic function assessed using Doppler tissue imaging in patients with hypertrophic cardiomyopathy: relation to symptoms and exercise capacity. *Heart* 2002;87:247-51.
 77. Solomon SD, Wolff S, Watkins H, et al. Left ventricular hypertrophy and morphology in familial hypertrophic cardiomyopathy associated with mutations of the beta-myosin heavy chain gene. *J Am Coll Cardiol* 1993;22:498-505.
 78. Ho CY, Sweitzer NK, McDonough B, et al. Assessment of diastolic function with Doppler tissue imaging to predict genotype in preclinical hypertrophic cardiomyopathy. *Circulation* 2002;105:2992-7.
 79. Araujo AQ, Arteaga E, Ianni BM, et al. Relationship between outflow obstruction and left ventricular functional impairment in hypertrophic cardiomyopa-

- thy: a Doppler echocardiographic study. *Echocardiography* 2006;23:734-40.
80. Bayrak F, Kahveci G, Mutlu B, et al. Tissue Doppler imaging to predict clinical course of patients with hypertrophic cardiomyopathy. *Eur J Echocardiogr* 2008;9:278-83.
 81. Weidemann F, Mertens L, Gewillig M, et al. Quantitation of localized abnormal deformation in asymmetric nonobstructive hypertrophic cardiomyopathy: a velocity, strain rate, and strain Doppler myocardial imaging study. *Pediatr Cardiol* 2001;22:534-7.
 82. Yang H, Sun JP, Lever HM, et al. Use of strain imaging in detecting segmental dysfunction in patients with hypertrophic cardiomyopathy. *J Am Soc Echocardiogr* 2003;16:233-9.
 83. Sengupta PP, Mehta V, Arora R, et al. Quantification of regional nonuniformity and paradoxical intramural mechanics in hypertrophic cardiomyopathy by high frame rate ultrasound myocardial strain mapping. *J Am Soc Echocardiogr* 2005;18:737-42.
 84. Pacileo G, Baldini L, Limongelli G, et al. Prolonged left ventricular twist in cardiomyopathies: a potential link between systolic and diastolic dysfunction. *Eur J Echocardiogr* 2011;12:841-9.
 85. Eyskens B, Ganame J, Claus P, et al. Ultrasonic strain rate and strain imaging of the right ventricle in children before and after percutaneous closure of an atrial septal defect. *J Am Soc Echocardiogr* 2006;19:994-1000.
 86. Di Salvo G, Drago M, Pacileo G, et al. Comparison of strain rate imaging for quantitative evaluation of regional left and right ventricular function after surgical versus percutaneous closure of atrial septal defect. *Am J Cardiol* 2005;96:299-302.
 87. Weidemann F, Eyskens B, Mertens L, et al. Quantification of regional right and left ventricular function by ultrasonic strain rate and strain indexes after surgical repair of tetralogy of Fallot. *Am J Cardiol* 2002;90:133-8.
 88. Knirsch W, Dodge-Khatami A, Kadner A, et al. Assessment of myocardial function in pediatric patients with operated tetralogy of fallot: preliminary results with 2D strain echocardiography. *Pediatr Cardiol* 2008;29:718-25.
 89. Salustri A, Kofflard MJ, Roelandt JR, et al. Assessment of left ventricular outflow in hypertrophic cardiomyopathy using any plane and paraplane analysis of three-dimensional echocardiography. *Am J Cardiol* 1996;78:462-8.
 90. Song JM, Fukuda S, Lever HM, et al. Asymmetry of systolic anterior motion of the mitral valve in patients with hypertrophic obstructive cardiomyopathy: a real-time three-dimensional echocardiographic study. *J Am Soc Echocardiogr* 2006;19:1129-35.
 91. Sitges M, Qin JX, Lever HM, et al. Evaluation of left ventricular outflow tract area after septal reduction in obstructive hypertrophic cardiomyopathy: a real-time 3-dimensional echocardiographic study. *Am Heart J* 2005;150:852-8.
 92. Qin JX, Shiota T, Asher CR, et al. Usefulness of real-time three-dimensional echocardiography for evaluation of myectomy in patients with hypertrophic cardiomyopathy. *Am J Cardiol* 2004;94:964-6.
 93. Anwar AM, Soliman OI, Geleijnse ML, et al. Assessment of left atrial ejection force in hypertrophic cardiomyopathy using real-time three-dimensional echocardiography. *J Am Soc Echocardiogr* 2007;20:744-8.
 94. Oe H, Hozumi T, Arai K, et al. Comparison of accurate measurement of left ventricular mass in patients with hypertrophied hearts by real-time three-dimensional echocardiography versus magnetic resonance imaging. *Am J Cardiol* 2005;95:1263-7.
 95. de Gregorio C, Recupero A, Grimaldi P, et al. Can transthoracic live 3-dimensional echocardiography improve the recognition of midventricular obliteration in hypertrophic obstructive cardiomyopathy? *J Am Soc Echocardiogr* 2006;19:1190.e1-4.
 96. Frans EE, Nanda NC, Patel V, et al. Live three-dimensional transthoracic contrast echocardiographic assessment of apical hypertrophic cardiomyopathy. *Echocardiography* 2005;22:686-9.
 97. Anwar AM, Nosir YFM, Zainal-Abidin SK, et al. Real-time three-dimensional transthoracic echocardiography in daily practice: initial experience. *Cardiovascular Ultrasound* 2012;10:14.
 98. Kelly NF, Platts DG, Burstow DJ. Feasibility of pulmonary valve imaging using three-dimensional transthoracic echocardiography. *J Am Soc Echocardiogr* 2010;23:1076-80.
 99. Anwar AM, Soliman O, van den Bosch AE, et al. Assessment of pulmonary valve and right ventricular outflow tract with real-time three-dimensional echocardiography. *Int J Cardiovasc Imaging* 2007;23:167-75.
 100. Rickers C, Wilke NM, Jerosch-Herold M, et al. Utility of cardiac magnetic resonance imaging in the diagnosis of hypertrophic cardiomyopathy. *Circulation* 2005;112:855-61.
 101. Flett AS, Westwood MA, Davies LC, et al. The prognostic implications of cardiovascular magnetic resonance. *Circ Cardiovasc Imaging* 2009;2:243-50.
 102. Choudhury L, Mahrholdt H, Wagner A, et al. Myocardial scarring in asymptomatic or mildly symptomatic patients with hypertrophic cardiomyopathy. *J Am Coll Cardiol* 2002;40:2156-64.
 103. Moon JC, McKenna WJ, McCrohon JA, et al. Toward clinical risk assessment in hypertrophic cardiomyopathy with gadolinium cardiovascular magnetic resonance. *J Am Coll Cardiol* 2003;41:1561-7.
 104. Dumont C, Monserrat L, Soler R, et al. Clinical significance of late gadolinium enhancement on cardiac magnetic resonance in patients with hypertrophic cardiomyopathy. *Rev Esp Cardiol* 2007;60:15-23.
 105. Adabag SA, Maron B, Appelbaum E, et al. Occurrence and frequency of arrhythmias in hypertrophic cardiomyopathy in relation to delayed enhancement on cardiovascular magnetic resonance. *J Am Coll Cardiol* 2008;51:1369-74.
 106. Vidal Perez RC, Pujadas S, Carreras F, et al. Myocardial fibrosis detected by delayed contrast-enhancement cardiovascular magnetic resonance relates with the incidence of atrial fibrillation in patients with hypertrophic cardiomyopathy. *Eur Heart J* 2008;29:494.
 107. Rubinshtein R, Glockne J, Ommen S, et al. Abstract 4187: Identification of late gadolinium enhancement by contrast-enhanced magnetic resonance imaging as a major risk factor for sudden death in hypertrophic cardiomyopathy. *AHA Scientific Sessions. Circulation* 2008;118:S-839.
 108. Hundley WG, Bluemke DA, Finn JP, et al. ACCF/ACR/AHA/NASCI/SCMR 2010 Expert Consensus Document on Cardiovascular Magnetic Resonance. A Report of the American College of Cardiology Foundation Task Force on Expert Consensus Documents. *Circulation* 2010;121:2462-2508.